

CrystEngComm

Accepted Manuscript



This is an *Accepted Manuscript*, which has been through the Royal Society of Chemistry peer review process and has been accepted for publication.

Accepted Manuscripts are published online shortly after acceptance, before technical editing, formatting and proof reading. Using this free service, authors can make their results available to the community, in citable form, before we publish the edited article. We will replace this *Accepted Manuscript* with the edited and formatted *Advance Article* as soon as it is available.

You can find more information about *Accepted Manuscripts* in the [Information for Authors](#).

Please note that technical editing may introduce minor changes to the text and/or graphics, which may alter content. The journal's standard [Terms & Conditions](#) and the [Ethical guidelines](#) still apply. In no event shall the Royal Society of Chemistry be held responsible for any errors or omissions in this *Accepted Manuscript* or any consequences arising from the use of any information it contains.



Temperature and electric field induced phase transition in [110]_c-oriented 0.63Pb(Mg_{1/3}Nb_{2/3})O₃-0.37PbTiO₃ single crystals

Wenhui He,^a Qiang Li,^a Nengneng Luo,^a Yiling Zhang^b and Qingfeng Yan^{*a}

Received 00th January 20xx,
Accepted 00th January 20xx

DOI: 10.1039/x0xx00000x

www.rsc.org/

Temperature-dependent domain configurations were studied for both unpoled and poled [110]_c-oriented 0.63Pb(Mg_{1/3}Nb_{2/3})O₃-0.37PbTiO₃ (PMN-0.37PT) single crystals by polarized light microscopy (PLM). Combining the dielectric properties and the domain configurations upon heating, it was found that the temperature-induced phase transition in unpoled [110]_c-oriented PMN-0.37PT single crystal followed the tetragonal (T) → cubic (C) sequence. However, under an electric (E) field of 10 kV/cm along [110]_c direction, a single domain orthorhombic (O) phase was induced. The E field-dependent domain structures were observed *in-situ* under PLM, which verified that the T phase turned to O phase when applied an E = 10 kV/cm along the [110]_c direction. Upon subsequent heating, the phase transition followed the O → T → C sequence. The O-T discontinuous phase transition led to a remarkable change in dielectric coefficient and strain with increasing temperature. The strain at 45°C (0.148%) was 2.2 times larger than that of at room temperature (0.068%), accompanied with a tremendous piezoelectric coefficients ($d_{33}^* \sim 1645$ pm/V).

1 Introduction

Over the past few decades, tremendous studies have focused on Pb(Mg_{1/3}Nb_{2/3})O₃-PbTiO₃ (PMN-PT) single crystals owing to their ultrahigh piezoelectric coefficient ($d_{33} > 2000$ pC/N) and electromechanical coupling factor ($k_{33} > 0.9$).¹⁻⁴ The polarization rotation was first proposed by Hu and Cohen in 2000 to explain the origin of excellent piezoelectric properties for ferroelectric single crystals.⁵ Generally, for PMN-xPT single crystals, the excellent electromechanical properties can be obtained around the morphotropic phase boundary (MPB) region, which is attributed to a flat free energy profile, leading to the low ferroelectric-ferroelectric phase transition temperature.^{6,7} However, the phase structure of a relaxor-PT single crystal with MPB composition is well known for its complication.⁸⁻¹² The existence of ferroelectric monoclinic (M) phase and orthorhombic (O) phase have been proved in both PMN-PT single crystals¹³⁻¹⁵ and ceramics^{16,17} with MPB compositions. The single domain structure of O phase (1O) could exist stably when the electric (E) field was applied along the [110]_c direction for relaxor-PT based single crystals at room temperature.^{14,18,19} Therefore, the O phase can be used to represent the phase structure of a PMN-PT single crystal near MPB after poling along the [110]_c direction at room temperature.

For piezoelectric crystals, an E-field poling is usually performed before application. Moreover, their thermal

stability is of concern for many applications.^{2,7} Perántie *et al.*²⁰ investigated the electric-field induced polarization rotation in [001]_c-poled PMN-PT single crystals, illustrating phase transition sequences from rhombohedral (R) phase to the tetragonal (T) phase through different monoclinic phases. Recently, complicated phase transitions induced by temperature and E field for PMN-0.35PT single crystal has been reported systematically by Zheng *et al.*²¹ Almost all of these studies focused on PMN-PT single crystals with R phase or just MPB compositions.²²⁻²⁵ However, the T phase relaxor-PT single crystals exhibit high Curie temperature compared with that of R phase and around the MPB.^{26,27} Most importantly, there is no ferroelectric-ferroelectric phase transition for T phase relaxor-PT single crystals, which expands the temperature usage range greatly.²⁷ Although the piezoelectric property of [001]_c-oriented T phase PMN-xPT single crystals was only about 300~400 pC/N,²⁶ these crystals with engineered domain configuration "2T" and "3T" theoretically should have high piezoelectric properties. Nevertheless, up to date, there is only few study on T phase PMN-xPT ($x \geq 0.36$), in particular on engineered domain configuration "2T" PMN-xPT ($x \geq 0.36$) single crystals. Moreover, the phase transition influenced by temperature and electric field for [110]_c-oriented PMN-xPT ($x \geq 0.36$) is still unclear.

Therefore, in this work, phase transition sequence of the [110]_c-oriented T-phase PMN-0.37PT single crystal induced by temperature and E field was identified. The domain structure variations induced by temperature or E field were observed intuitively via *in-situ* polarized light microscope (PLM) observation along pseudo-cubic [110]_c direction of unpoled PMN-0.37PT single crystal. The properties evolution associated

^a Department of Chemistry, Tsinghua University, Beijing 100084, China. E-mail: yanqf@mail.tsinghua.edu.cn; Tel: +86 10 62792830

^b State Key Laboratory of New Ceramics and Fine Processing, Tsinghua University, Beijing 100084, China.

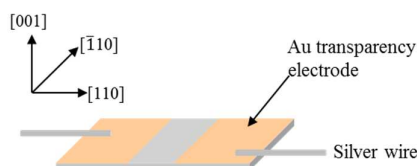


Fig. 1 The schematic diagram of the sample for observing electric-field induced domain evolution by PLM. The electrodes were sputtered along the $[110]_C$ on the $(100)_C$ surface.

with the phase transition process was systematically studied. It was found that the temperature induced a $T \rightarrow$ cubic (C) phase transition in unpoled $[110]_C$ -oriented PMN-0.37PT single crystal, while it induced a $O \rightarrow T \rightarrow C$ phase transition in poled single crystal. Furthermore, the O - T discontinuous phase transition in poled single crystal led to a remarkable change in dielectric coefficient and strain with increasing temperature, accompanied with a tremendous piezoelectric coefficient ($d_{33}^* \sim 1645$ pm/V).

2 Experimental

The PMN-0.37PT single crystals used in this work were grown by a modified Bridgman method.³ Crystal samples were cut from the top of the as-grown boule, and oriented using X-ray crystal diffraction instrument (DX-2/4A). Then, samples were cut and finely polished with one pair of parallel surfaces along the $[110]_C$ direction for domain observation by a polarized light microscope (XJZ-6) connected to a computer and equipped with a hot stage (Linkam, THMS600). The $[110]_C$ E field induced domain evolution was observed on the $(001)_C$ surface. The schematic diagram for the observation of domain evolution induced by E field is illustrated in Fig. 1. Other samples for properties test were poled by 10 kV/cm E field for 2 min in silicon oil at room temperature. Temperature-dependent dielectric constants were measured by an Agilent 4294A impedance analyzer connected with a Delta 9023 temperature control system. X-ray diffraction analysis was determined using an X-ray diffractometer (D8 ADVANCE) with Cu K_α radiation to verify the crystal structure. The E field-induced strain was measured at a frequency of 1 Hz and variable temperatures using a TF Analyzer 2000 (aixACCT).

3 Results and discussion

3.1 Phase transition in unpoled $[110]_C$ -oriented PMN-PT single crystal induced by temperature

Fig. 2 depicts the temperature dependence of dielectric constant and dielectric loss for unpoled $[110]_C$ -oriented PMN-xPT single crystals. From Fig. 2, it can be seen that exclusive step-like anomaly at 175°C should be associated with the Curie temperature. According to the following equation:²⁶

$$x = \frac{T_c + 59^\circ\text{C}}{631^\circ\text{C}} \quad (x < 0.457) \quad (1)$$

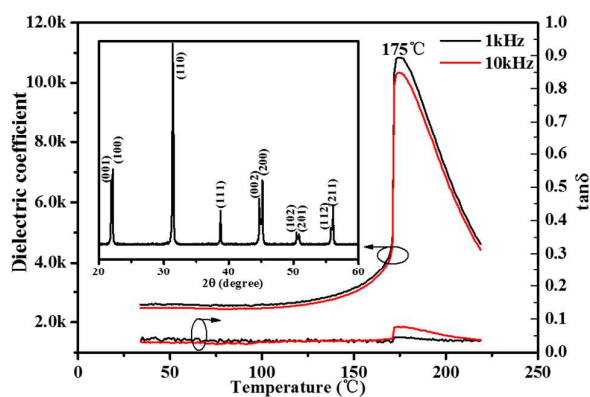


Fig. 2 Temperature-dependent dielectric constant and dielectric loss for unpoled $[110]_C$ -oriented PMN-xPT single crystal at 1 and 10 kHz. The inset shows XRD pattern of crushed PMN-xPT crystal powders.

$x=0.37$ was calculated, demonstrating the unpoled $[110]_C$ -oriented PMN-0.37PT crystals located in the T phase region at room temperature. Hence, the phase transition of $[110]_C$ -oriented PMN-0.37PT induced by temperature underwent T phase to C phase. It should be noted that at 1 kHz and 10 kHz the dielectric loss was only about 0.045% at room temperature, which could be attributed to the fewer domain walls.²⁸ The XRD pattern was presented in inset of Fig. 2, which further demonstrated that it was a typical T phase crystal.^{29,30}

In general, for tetragonal crystals, there are six spontaneous polarization (P_s) existing along crystallographic directions $\langle 001 \rangle$, as depicted in Fig. 3. According to the geometrical relationship between P_s and its projection on the $(001)_C$, $(110)_C$ and $(\bar{1}10)_C$ surfaces, the domain walls of 90° domain on the (110) surface are along the $[\bar{1}11]_C$ or $[1\bar{1}1]_C$ direction. In other words, the angle θ between the 90° domain walls and the edge of the single crystal sample is 45° . However, 180° domain walls on the (110) plane can't be detected by PLM due to polarized light has equivalent response to 180° domain. On this occasion, domain walls could not be observed.

To further verify the phase structure of the selected crystal, the temperature-dependent domain structure was investigated. Fig. 4 presents the domain structure changes at the crossed polarized/analyzer (P/A): 45° when temperature varied. According to the extinction rules of T-phase $[110]_C$ -oriented PMN-PT, it should be bright at P/A: 45° . On the contrary, it occurred extinction at P/A: 0° (the inset of Fig. 4(a)). As shown in Fig. 4(a), at 30°C , the domain size is about $100 \mu\text{m}$, indicating a high degree of long-range order of B-Site in ABO_3 perovskite structure, which also proves that the specimen is in T phase region.³¹ It can be seen that on the $(110)_C$ surface the domain walls of 90° domain are along $[1\bar{1}1]_C$ direction, which is consistent with the domain walls between P_{s1} and P_{s3} . Moreover, the angle between the $[\bar{1}10]_C$ margin and the domain walls observed is about 45° . Furthermore, it should be noted that it was not a perfect extinction at P/A: 0° as shown in the inset of Fig. 4(a), which was associated with the reflection of light from the domain walls or the presence of elastic energy. However, the

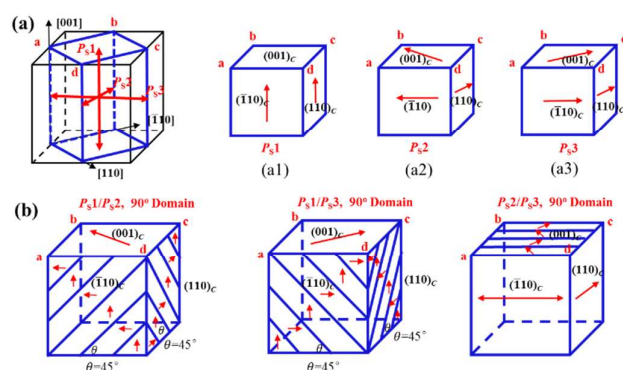


Fig. 3 Schematics of (a) Six equivalent spontaneous polarizations of T phase and the projections of (a1) P_{s1} , (a2) P_{s2} and (a3) P_{s3} on the $(001)_c$, $(110)_c$ and $(\bar{1}10)_c$ surfaces, respectively and (b) domain walls between P_{s1} and P_{s2} , P_{s1} and P_{s3} , P_{s2} and P_{s3} . The letters (a, b, c, d) are used as fixed-point notation.

interference colour gradually changed at $P/A:45^\circ$, which may be related to the domain walls vibration and domain walls translation induced by temperature.

With increasing temperature, the domain size and domain wall numbers had no obvious changes, indicating that there was no ferroelectric-ferroelectric phase transition prior to Curie temperature. When the temperature increased to 173°C , the new phase showed extinction for all θ from 0° to 360° , indicating the formation of the C phase, as shown in Fig. 4(f). At 175°C , the crystal became paraelectric phase, and it was all dark in sight. Based on the

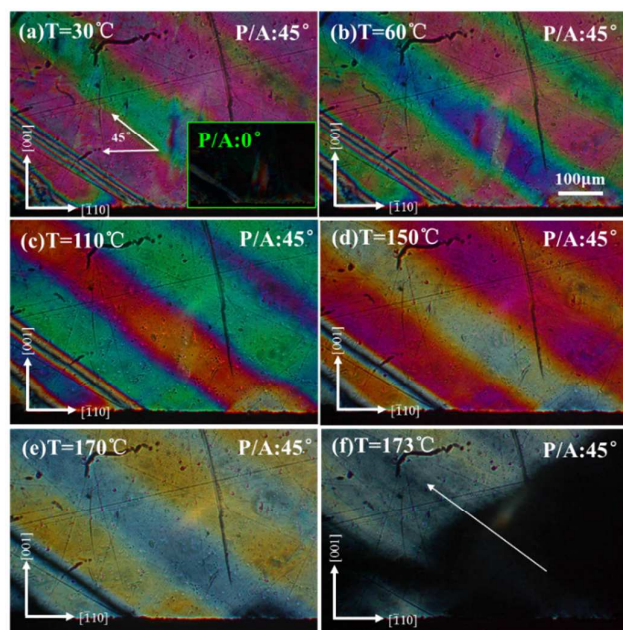


Fig. 4 Domain structure vs. temperature at $P/A:45^\circ$ for unpoled $[110]_c$ -oriented PMN-0.37PT single crystal by *in-situ* PLM observation (a) 30°C , (b) 60°C , (c) 110°C , (d) 150°C , (e) 170°C , and (f) 173°C . The inset of (a) shows the domain structure at $P/A:0^\circ$. The arrow in (f) indicates the direction of the cubic phase formation.

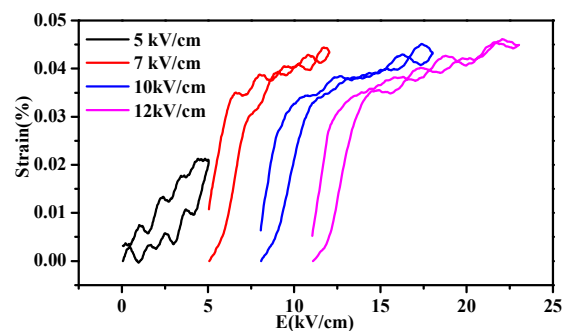


Fig. 5 Strain vs electric field behaviors for the poled $[110]_c$ -oriented PMN-0.37PT crystal with various electric fields.

temperature-dependent dielectric properties and domain configurations, it demonstrated that the phase transition sequence of unpoled $[110]_c$ -oriented PMN-0.37PT was T phase to C phase induced by temperature.

3.2 Phase transition in unpoled $[110]_c$ -oriented PMN-PT single crystal induced by electric field

To illustrate that the phase transition behavior under an E field applying along the $[110]_c$ direction was different from that by temperature, the electric field-induced strain behavior for $[110]_c$ -oriented PMN-0.37PT crystal was investigated at room temperature, as shown in Fig. 5. Interestingly, it can be observed that for T-phase crystals a small E field of 5 kV/cm was not enough to span the energy barrier between the T phase and O phase. When an electric field $E = 7$ kV/cm was applied, $P_s[001]_c$ of T phase would begin to overcome the potential barrier and switched to $P_s[110]_c$ of O phase. Therefore, the O phase was induced due to the applied E field being parallel to the spontaneous polar direction $[110]_c$ of O phase. Thus, when applied an E field of 10 kV/cm along $[110]_c$ to pole the sample, the O phase was induced from T phase. The unipolar strain (S_{uni} -E) loops shown in Fig. 5 demonstrated that the unpoled $[110]_c$ -oriented PMN-0.37PT would undergo a phase transition from T phase to O phase induced by E field at room temperature.

In order to figure out the phase transition induced by E field intuitively, *in-situ* PLM observation was carried out with different applied E fields. As schematically depicted in Fig. 6, with the E field increasing, re-orientation of the spontaneous polarization leads to the domain structure variation from 6T to 2T, and finally to 1O single domain structure. Accordingly, the extinction behaviour also changes at $P/A:0^\circ$, as schematically shown in Fig. 6(b). In theory, when the crystal becomes a 1O single domain structure (Fig. 6(b)), the sample should occur extinct at $P/A:0^\circ$.

The E field-dependent domain structure at $P/A:0^\circ$ was observed *in situ* by using PLM. As shown in Fig. 1, the electric field was along the $[110]_c$ direction. In theory, before the application of the E field, the sample should be bright at $P/A:0^\circ$. In fact, as shown in Fig. 7(a), the intensity of the transmitted light reached the maximum at $P/A:0^\circ$. In other words, it was the brightest at all angles. This result was consistent with the theoretical prediction in Fig. 6(b) very well. And then, we observed the domain variation at $P/A:0^\circ$ under different E fields. When the E field was 5 kV/cm, there had no

obvious change as shown in Fig. 7(b), which indicated that the 2T engineered domain formed. While, as the E field increased to 7 kV/

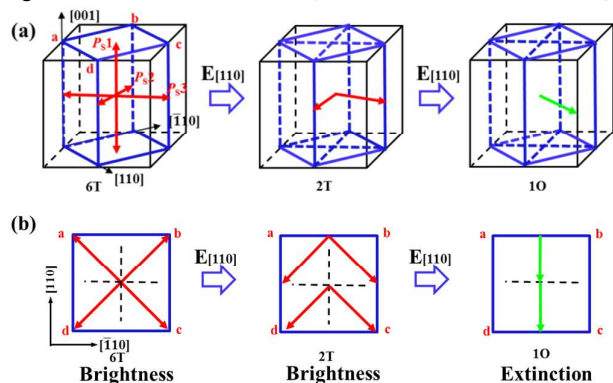


Fig. 6 Schematics of (a) the change of the spontaneous polarization and (b) the extinction rule variation with E field increasing for $[110]_c$ -oriented PMN-0.37PT single crystal. The letters (a, b, c, d) are used as fixed-point notation.

cm, the spontaneous polarizations $P_s [001]_c$ of T phase got closer to $P_s [110]_c$ of O phase. The 1O single domain phase began to develop gradually in the T matrix, corresponding to the small extinction region in Fig. 7(c). As the E field further increased to 8 kV/cm, the extinction area was enlarged (Fig. 7(d)). With further increasing the E field, it was totally extinct, suggesting the 1O single domain phase formed for the whole sample when the $E \geq 10$ kV/cm, as shown in Fig. 7(e) and (f). These results were consistent with the E field-dependent strain discussed above very well.

From the E field dependence of domain structures variation analysed above, it can be concluded that the phase transition sequence of the unpoled $[110]_c$ -oriented PMN-0.37PT single crystal under the $[110]_c$ direction E field was from T phase to O phase, which was different from that induced by temperature.

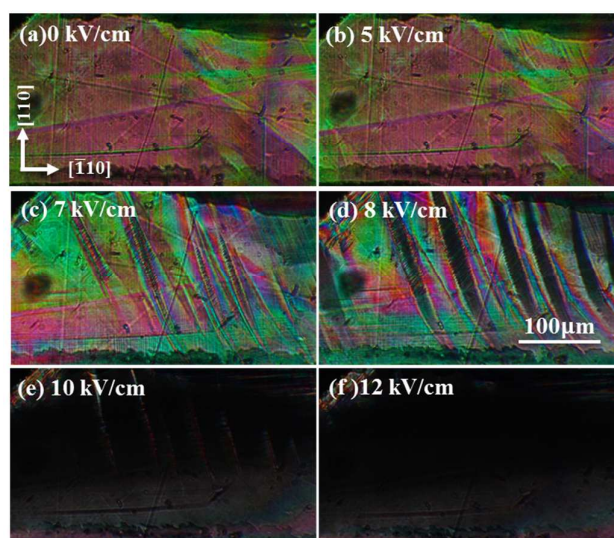


Fig. 7 Domain structures at P/A:0° under different E fields along $[110]_c$ direction at room temperature: (a) $E = 0$ kV/cm, (b) $E = 5$ kV/cm, (c) $E = 7$ kV/cm, (d) $E = 8$ kV/cm, (e) $E = 10$ kV/cm, and (f) $E = 12$ kV/cm.

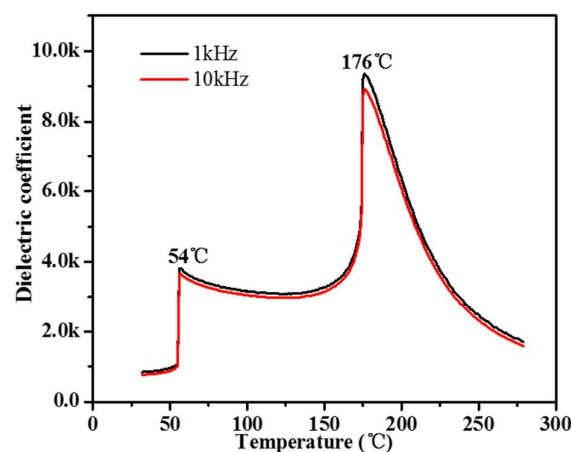


Fig. 8 Temperature dependence of dielectric constant and dielectric loss for poled $[110]_c$ -oriented PMN-37PT single crystal at 1 and 10 kHz.

3.3 Phase transition in $[110]_c$ -oriented PMN-PT single crystal induced by E field and temperature

To investigate the phase transition of poled specimen influenced by temperature, the temperature-dependent dielectric properties for poled $[110]_c$ -oriented PMN-0.37PT single crystal was measured, as shown in Fig. 8. According to the electric field induced phase transition demonstrated in Fig. 5 and Fig. 6, a 1O domain configuration could be obtained in a poled sample. What's more, the single domain state is liable to interference by temperature.³² Hence, the single domain O phase should be substituted at higher temperatures. The ferroelectric-ferroelectric phase transition at 54°C shown in Fig. 8 should be O to T phase transition, demonstrating that the induced O phase depolarized to T phase under the disturbance of high temperature. The T phase is maintained upon further heating until 176°C. Based on the analysis, it can be confirmed that the poling electric field ($E = 10$ kV/cm) had induced the phase transition from 2T phase to 1O phase at room temperature, and then was degraded to T phase at higher temperature. Meanwhile, corresponding changes in dielectric coefficient influenced by temperature could be observed. It is noteworthy that the ϵ_{33} of the single domain O phase at room temperature was about 840, which was in accordance with the value reported by Zheng *et al.*²¹

To evaluate the thermal stability of property under an E field, the S_{uni} -E patterns at 10 kV/cm at various temperatures for $[110]_c$ -oriented PMN-0.37PT single crystal were measured. Fig. 9(a) indicates that the T phase sample was induced to the single domain O phase under the electric field of 10 kV/cm at 30°C. It should be noted that the behavior shown in Fig. 9(a) is nearly a continuous phase transition. As a rule, the same polarization forms small regions defined domains, which is separated by the domain walls. Each domain has a different transition threshold and is assumed to undergo an ideal discontinuous transition between ferroelectric phases.³³ In this work, each domain transformed to 1O single domain at 30°C from 2T engineered domain with a different

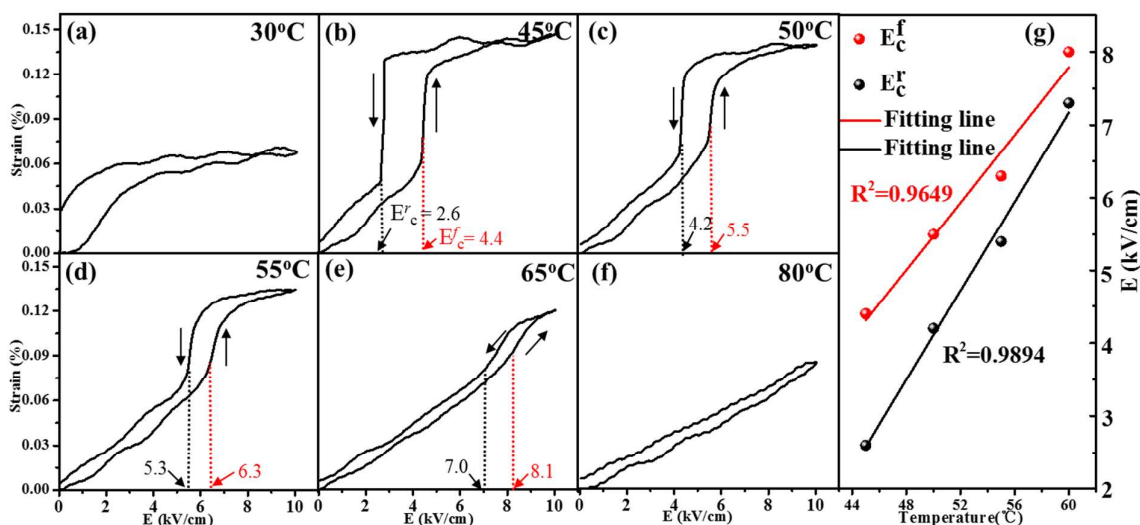


Fig. 9 (a)-(f) The unipolar strain (S_{uni-E}) plots as a function of temperature for $[110]_C$ -oriented PMN-0.37PT single crystal. (g) Temperature-dependent phase transition threshold from T phase to O phase (E_c^f) and O phase to T phase (E_c^r).

transition threshold. Therefore, from a macro point of view, it was a continuous phase transition at 30°C. As the temperature increasing, Fig. 9(b) displays a discontinuous phase transition, indicating that the sample was nearly single domain at 45°C. Correspondingly, the strain increased enormously. The strain value was 0.148% at 45°C, which was 2.2 times larger than 0.068% at ambient temperature.

As pointed out by J.A. Gallagher et al., the coercive field E_c^f in Fig. 9(b) stands for the forward E field that drives the phase transition from T to O phase, and the E_c^r represents required reverse electric field for the O to T phase transition.³⁴ The values of E_c^f and E_c^r were 4.4 kV/cm and 2.6 kV/cm at 45°C, respectively. As temperature continued to rise, the two values both increased regularly. As shown in Fig. 9(g), good linearity between temperature and the phase transition E field existed by fitting when the samples was heated, which indicated that temperature had a major impact on the phase transition at 10 kV/mm electric field. The relationship of E_c^f and E_c^r with temperature (T) can be described as following:

$$E_c^f = 0.247T - 6.5 \quad (2)$$

$$E_c^r = 0.307T - 10.3 \quad (3)$$

From the relation formula (2), at room temperature (30°C), the E_c^f is calculated about 0.7 kV/cm, meaning a minimum E field threshold of 0.7kV/cm is required for one domain phase transition from T phase to O phase. Hence, at 30°C, the phase transition threshold from T phase to O phase for the whole sample is much greater than 0.7kV/cm. Therefore, When applying the E field (10 kV/cm) along the $[110]_C$ direction, the continuous phase transition shown in Fig. 9(a) occurred. According to formula (3), E_c^r is determined to be -1.3 kV/cm ($E_c^r < 0$) at 30°C, which means that at this temperature the phase transition from O phase to T phase doesn't exist in $[110]_C$ -oriented PMN-0.37PT single crystal. The formula (2) and (3) were obtained at 10 kV/cm under different temperature. That is to say, the energy supplied by the E field to induce T phase to O phase is constant. Note that at a high

temperature, it is conducive to the existence of T phase,³⁵ resulting in the higher energy potential barrier between T phase and O phase, which leads to the more difficult phase transition between the $[110]_C$ -oriented T phase and the induced O phase. With the rising of temperature, the energy supplied by the E field was little by little and not enough to span the energy potential barrier influenced by temperature. Therefore, further increasing the temperature ($T > 68^\circ\text{C}$), the E_c^f calculated from formula (2) exceeded 10kV/cm. So the phase transition from T phase to O phase didn't exist, as shown in Fig. 9(f). It is comprehensible that the E_c^f and E_c^r in one specimen both increased upon heating (45°C ~ 65°C), due to elevated energy potential barrier at higher temperature. Another perspective to the issue, when the T phase to O phase doesn't occur, the O phase to T phase would not happen. Hence, the special phase transition for $[110]_C$ -oriented PMN-0.37PT single crystal exists in a temperature range.

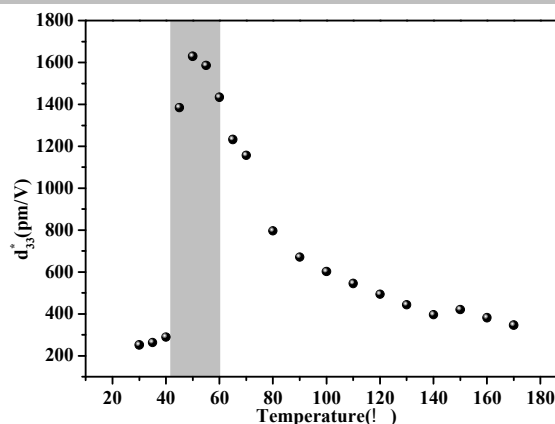


Fig. 10 Temperature dependences of piezoelectric constants (d_{33}) obtained from unipolar strain.

The piezoelectric property is an important parameter for ferroelectric crystals. Therefore, the d_{33}^* values derived from the E field-induced strain at different temperature are shown in Fig. 10. Based on the above results, the single O phase was induced from T phase after poled along the $[110]_C$ direction at 10 kV/cm. It has been reported that for single domain structure, the polarization extension occurs and it has no polarization rotation,² leading to a relatively low piezoelectric coefficient (~ 220 pm/V). With temperature increasing, the 2T phase was induced through the depolarization. What is noteworthy is that in this phase transition region marked in the dark area of Fig. 10, the piezoelectric coefficient increased significantly with a maximum $d_{33}^* \sim 1645$ pm/V, which could be attributed to the domain walls motion and polarization rotation in 2T engineered domain configurations crystals. The piezoelectric coefficients decreased gradually at elevated temperature, which was associated with dipole moment decreasing for T phase crystal.

Conclusions

In summary, we have demonstrated that temperature and electric field induce different phase transition sequence for $[110]_C$ -oriented PMN-0.37PT. Temperature-dependent dielectric properties and domain structures observed via *in-situ* PLM for unpoled $[110]_C$ -oriented PMN-0.37PT indicated that the phase transition followed the T \rightarrow C sequence induced by temperature. While, the phase transition from T phase to O phase was induced by E field ($E = 10$ kV/cm) along the $[110]_C$ direction at room temperature. And upon further heating, the phase transition followed the O \rightarrow T \rightarrow C sequence. What's more, the O to T discontinuous phase transition led to a remarkable change in dielectric constant and strain with increasing temperature. The strain at 45 °C (0.148%) was 2.2 times larger than that at room temperature (0.068%), accompanied with a tremendous piezoelectric coefficient ($d_{33}^* \sim 1645$ pm/V).

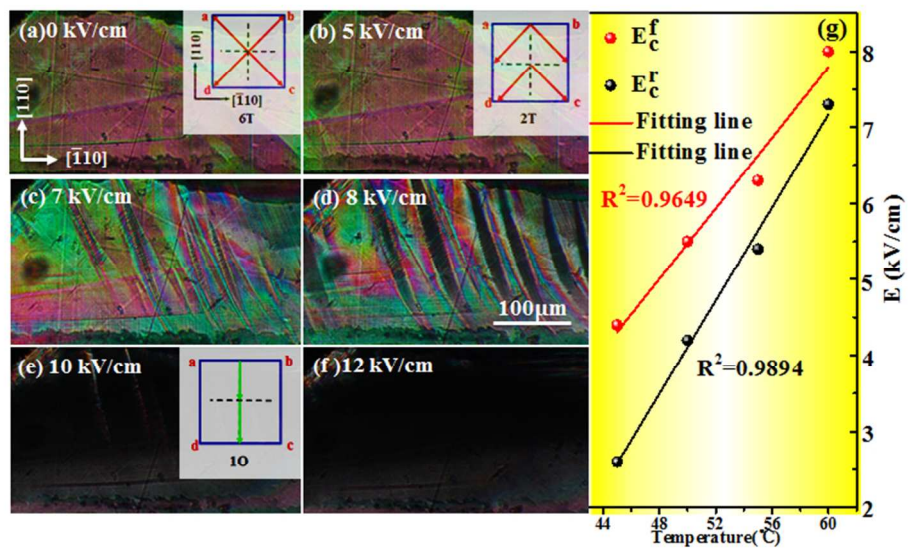
Acknowledgements

This work was supported by the National Basic Research Program of China (Grant No. 2013CB632900), the National Natural Science Foundation of China (Nos. 50972071, 51172118 and 91333109). The Tsinghua University Initiative Scientific Research Program and the State Key Laboratory of New Ceramics and Fine Processing, Tsinghua University are also acknowledged for partial financial support.

References

- 1 S. E. Parka and T. R. Shrout, *J. Appl. Phys.*, 1997, **82**, 1804.
- 2 S. Zhang and F. Li, *J. Appl. Phys.*, 2012, **111**, 031301.
- 3 N. Luo, Y. Li, Z. Xia and Q. Li, *CrystEngComm*, 2012, **14**, 4547.
- 4 H. Luo, G. Xu, P. Wang and Z. Yin, *Ferroelectrics*, 1999, **231**, 685.
- 5 H. Fu and R. E. Cohen, *Nature*, 2000, **403**, 281.
- 6 F. Li, L. Jin, Z. Xu, D. Wang, S. Zhang, *Appl. Phys. Lett.*, 2013, **102**, 152910.

- 7 W. He, Q. Li, Q. Yan, N. Luo, Y. Zhang, X. Chu, D. Shen, *Crystals*, 2014, **4**, 262.
- 8 M. Ahart, M. Somayazulu, R. Cohen, P. Ganesh, P. Dera, H. K. Mao, R. J. Hemley, Y. Ren, P. Liermann and Z. Wu, *Nature*, 2008, **451**, 545.
- 9 W. Cao and L. E. Cross, *Phys. Rev. B*, 1993, **47**, 4825.
- 10 D. Damjanovic, *Appl. Phys. Lett.*, 2010, **97**, 062906.
- 11 C. He, X. Li, Z. Wang, Y. Liu, D. Shen, T. Li and X. Long, *CrystEngComm*, 2012, **14**, 4513.
- 12 D. La-Orauttapong, B. Noheda, Z. Ye, P. M. Gehring, J. Toulouse, D. E. Cox, and G. Shirane, *Phys. Rev. B*, 2002, **65**, 144101.
- 13 Z. Ye, B. Noheda, M. Dong, D. Cox and G. Shirane, *Phys. Rev. B*, 2001, **64**, 184114.
- 14 Y. Lu, D. Y. Jeong, Z. Y. Cheng, Q. M. Zhang, H. Luo, Z. Yin and D. Viehland, *Appl. Phys. Lett.*, 2001, **78**, 3109.
- 15 J. Qiu, J. Ding, N. Yuan and X. Wang, *J. Appl. Phys.*, 2015, **117**, 074101.
- 16 B. Noheda, D. E. Cox, G. Shirane, J. Gao and Z. Ye, *Phys. Rev. B*, 2002, **66**, 054104.
- 17 A. K. Singh and D. Pandey, *Phys. Rev. B*, 2003, **67**, 064102.
- 18 S. Zhang, G. Liu, W. Jiang, J. Luo, W. Cao and T.R. Shrout, *J. Appl. Phys.*, 2011, **110**, 064108.
- 19 H. Deng, X. Zhao, H. Zhang, C. Chen, X. Li, D. Lin, B. Ren, J. Jiao and H. Luo, *CrystEngComm*, 2014, **16**, 2760.
- 20 J. Peräntie, J. Hagberg, A. Uusimäki, J. Tian and P. Han, *J. Appl. Phys.*, 2012, **112**, 034117.
- 21 L. Zheng, X. Lu, H. Shang, Z. Xi, R. Wang, J. Wang, P. Zheng and W. Cao, *Phys. Rev. B*, 2015, **91**, 184105.
- 22 Z. Wang, R. Zhang, E. Sun and W. Cao, *J. Mater. Sci.*, 2012, **47**, 429.
- 23 Q. Lu, X. Long and Y. Hu, *CrystEngComm*, 2010, **12**, 4317.
- 24 A. K. Singh and D. Pandey, *Phys. Rev. B*, 2003, **67**, 064102.
- 25 R. Zhang, W. Jiang and W. Cao, *Appl. Phys. Lett.*, 2005, **87**, 182903.
- 26 F. Li, S. Zhang, Z. Xu, X. Wei, J. Luo and T.R. Shrout, *J. Appl. Phys.*, 2010, **108**, 034106.
- 27 D. Lin, S. Zhang, Z. Li, F. Li, Z. Xu, S. Wada, J. Luo, T.R. Shrout, *J. Appl. Phys.*, 2011, **110**, 084110.
- 28 D. Lin, Z. Li, F. Li and S. Zhang, *CrystEngComm*, 2013, **15**, 6292.
- 29 N. Luo, S. Zhang, Q. Li, Q. Yan, W. He, Y. Zhang and T. R. Shrout, *Appl. Phys. Lett.*, 2014, **104**, 182911.
- 30 Y. Liu, X. Li, Z. Wang, C. He, T. Li, L. Ai, T. Chu, D. Pang and X. Long, *CrystEngComm*, 2013, **15**, 1643.
- 31 C. A. Randall, A. S. Bhalla, T. R. Shrout and L.E.Cross, *J. Mater. Res.*, 1990, **5**, 829.
- 32 F. Li, L. Wang, L. Jin, Z. Xu and S. Zhang, *CrystEngComm*, 2014, **16**, 2892.
- 33 K. G. Webber, H. C. Robinson, G. A. Rossetti Jr. and C. S. Lynch, *Acta Materialia*, 2008, **56**, 2744.
- 34 J.A. Gallagher, C.S. Lynch, *Proceedings of the ASME 2013 Conference on Smart Materials, Adaptive Structures and Intelligent Systems*, 2013, **SMASIS2013-3279**.
- 35 M. Davis, D. Damjanovic, N. Setter, *Phys. Rev. B*, 2006, **73**, 014115.



290x170mm (72 x 72 DPI)